JOURNAL OF VIROLOGY, Mar. 1997, p. 2425–2435 Vol. 71, No. 3
0022-538X/97/$04.00+0

The Transneuronal Spread Phenotype of Herpes Simplex Virus Type 1 Infection of the Mouse Hind Footpad

JEFFREY P. ENGEL,[1]* TIMOTHY C. MADIGAN,[1] AND GARY M. PETERSON[2]

Departments of Medicine[1] and Anatomy and Cell Biology,[2] East Carolina University School of Medicine, Greenville, North Carolina 27858

Received 5 September 1996/Accepted 20 November 1996

The mouse hind footpad inoculation model has served as a standard laboratory system for the study of the neuropathogenesis of herpes simplex virus type 1 (HSV-1) infection. The temporal and spatial distribution of viral antigen, known as the transneuronal spread phenotype, has not previously been described; nor is it understood why mice develop paralysis in an infection that involves sensory nerves. The HSV-as-transneuronal-tracer experimental paradigm was used to define the transneuronal spread of HSV-1 in this model. A new decalcification technique and standard immunocytochemical staining of HSV-1 antigens enabled a detailed analysis of the time-space distribution of HSV-1 in the intact spinal column. Mice were examined on days 3, 4, 5, and 6 postinoculation (p.i.) of a lethal dose of wild-type HSV-1 strain 17 *syn*$^+$. Viral antigen was traced retrograde into first-order neurons in dorsal root ganglia on day 3 p.i., to the dorsal spinal roots on days 4 and 5 p.i., and to second- and third-order neurons within sensory regions of the spinal cord on days 5 and 6 p.i. HSV-1 antigen distribution was localized to the somatotopic representation of the footpad dermatome within the dorsal root ganglia and spinal cord. Antigen was found in the spinal cord gray and white matter sensory neuronal circuits of nociception (the spinothalamic tract) and proprioception (the dorsal spinocerebellar tract and gracile fasciculus). Within the brain stems and brains of three paralyzed animals examined late in infection (days 5 and 6 p.i.), HSV antigen was restricted to the nucleus subcoeruleus region bilaterally. Since motor neurons were not directly involved, we postulate that hindlimb paralysis may have resulted from intense involvement of the posterior column (gracile fasciculus) in the thoracolumbar spinal cord, a region known to contain the corticospinal tract in rodents.

Herpes simplex virus (HSV) infection, like all alphaherpesvirus infections of mammals, is characterized by nervous system involvement after inoculation at a peripheral site, usually at the skin or mucus membranes. The ability of HSV to invade the nervous system directly from the portal of entry was first demonstrated in experimental animals by Goodpasture and Teague (11) and confirmed later in numerous studies (7, 14, 17, 18, 36). These studies demonstrated convincingly the neurotropic properties of alphaherpesviruses and their abilities to cause lesions and to spread within specific neural routes.

Early investigations of herpetic neurotropism relied upon descriptive pathology as the phenotypic expression of viral infection. The experimental paradigm consisted of inoculating an animal at a peripheral site, such as the nose or eye, sacrificing the animal days later when clinical disease developed, and identifying areas in the central nervous system (CNS), usually the brain, with obvious virus-induced neuropathology (11, 14, 17, 18, 36). Later studies refined this experimental approach by describing a neuroinvasiveness phenotype determined by measuring viral growth within tissues. Thus, in the study of acute HSV infection, the neuroinvasiveness phenotype was measured by comparing in vivo viral replication kinetics at the site of inoculation to the subserving neural tissue (7, 30). Because viral mutants with diminished neuroinvasiveness existed (13, 37) with viral growth of several orders of magnitude less within neural tissue, these experiments proved useful in the discovery of viral gene products required for wild-type neurovirulence (13, 30, 37).

* Corresponding author. Mailing address: Department of Medicine, East Carolina University School of Medicine, 600 Moye Blvd., Greenville, NC 27858. Phone: (919) 816-2550. Fax: (919) 816-3472. E-mail: engel@brody.med.ecu.edu.

Recently, a new experimental paradigm to describe alphaherpesvirus neuropathogenesis has emerged. Because of their intra-axonal anterograde and retrograde spread, transsynaptic specificity, and replication within the neuronal perikarya which amplifies viral antigen signal, alphaherpesviruses were found to be ideal for tracing neuronal circuitry in vivo by immunocytochemical and light-microscopic techniques (1, 2, 16, 20, 24, 32–34). These viruses have become preferred over traditional transneuronal tracers, such as horseradish peroxidase, because their signals can be traced transsynaptically to higher-order neurons (20, 32, 33) after inoculation at the periphery. Thus, HSV and pseudorabies virus (PrV) have been used to delineate many sensory, motor, and autonomic neuroanatomical connections in a variety of mammalian species (1, 2, 4, 5, 16, 19, 24, 32–34). The alphaherpesvirus-as-transneuronal-tracer system has been adapted and used successfully to measure the virologic phenotype known as the transneuronal spread phenotype (4, 5, 16, 32–34). The tracer paradigm, complementing the neuroinvasiveness phenotype of alphaherpesvirus infection, offers the potential of comparative viral replication kinetic analysis of the routes of neuronal spread within the host by using both the wild type and genetically mapped viral mutants.

The mouse has emerged as a preferred species for models of acute infection because it is a permissive host and is easily manipulated in the laboratory setting. Inoculation of virus onto the hind footpad has proved to be a very predictable portal of entry for measurements of neuroinvasiveness (7, 9, 10, 13, 14, 17–19, 21, 36, 37), and this model is a reasonably close approximation to acute primary infection in humans which also involves the skin and sensory nerves. After infection of the mouse hind footpad with a lethal dose of wild-type HSV type 1 (HSV-1), disease is characterized by the development of

TABLE 1. Summary of strain 17 *syn*$^+$ inoculations

Animal no.	Inoculum (PFU)	Day p.i.	Hindlimb paralysis[a]
1	4×10^6	3	−
2	3×10^7	3	−
3	3×10^7	3	−
4	3×10^7	4	−
5	3×10^7	4	−
6	3×10^7	4	−
7	3×10^7	5	−
8	3×10^7	5	−
9	3×10^7	5	−
10	8×10^7	5	+
11	8×10^7	6	+
12	8×10^6	6	+

[a] +, paralysis; −, no paralysis.

hindlimb paralysis 5 to 7 days postinoculation (p.i.) and death from an ascending encephalomyelitis by day 10 p.i. Neuroinvasiveness is demonstrated by efficient viral replication in the sciatic nerve, dorsal root ganglia, spinal cord, and brain in relation to viral growth in the footpad (7, 10, 13, 36, 37).

Despite the extensive use of this model of infection, little is known about the temporal and spatial distribution, that is, the transneuronal spread, of viral infection in the peripheral nervous system and CNS. Of fundamental interest is to understand why mice develop motor nerve symptoms (paralysis) after viral inoculation onto the skin which leads to infection of sensory nerve pathways. It is not known if motor involvement results from transneuronal spread from sensory regions to motoneurons within the spinal cord, brain stem, or brain or, alternatively, from nonsynaptic mechanisms within the CNS.

To address these questions, we used the alphaherpesvirus-as-transneuronal-tracer experimental paradigm (20) to define the transneuronal spread phenotype of wild-type HSV-1 infection in the mouse hind footpad inoculation system. We used this approach to provide a roadmap of the route of viral spread within the CNS of the mouse, tracing viral antigen into the spinal cords and brains of infected animals.

MATERIALS AND METHODS

Virus strain and tissue culture. HSV-1 strain 17 *syn*$^+$ (10) was used for all animal inoculations. In vitro, virus was passaged on rabbit skin cells maintained in minimal essential medium supplemented with 10% fetal calf serum and antibiotics. High-titer viral stock was prepared by concentrating infected rabbit skin

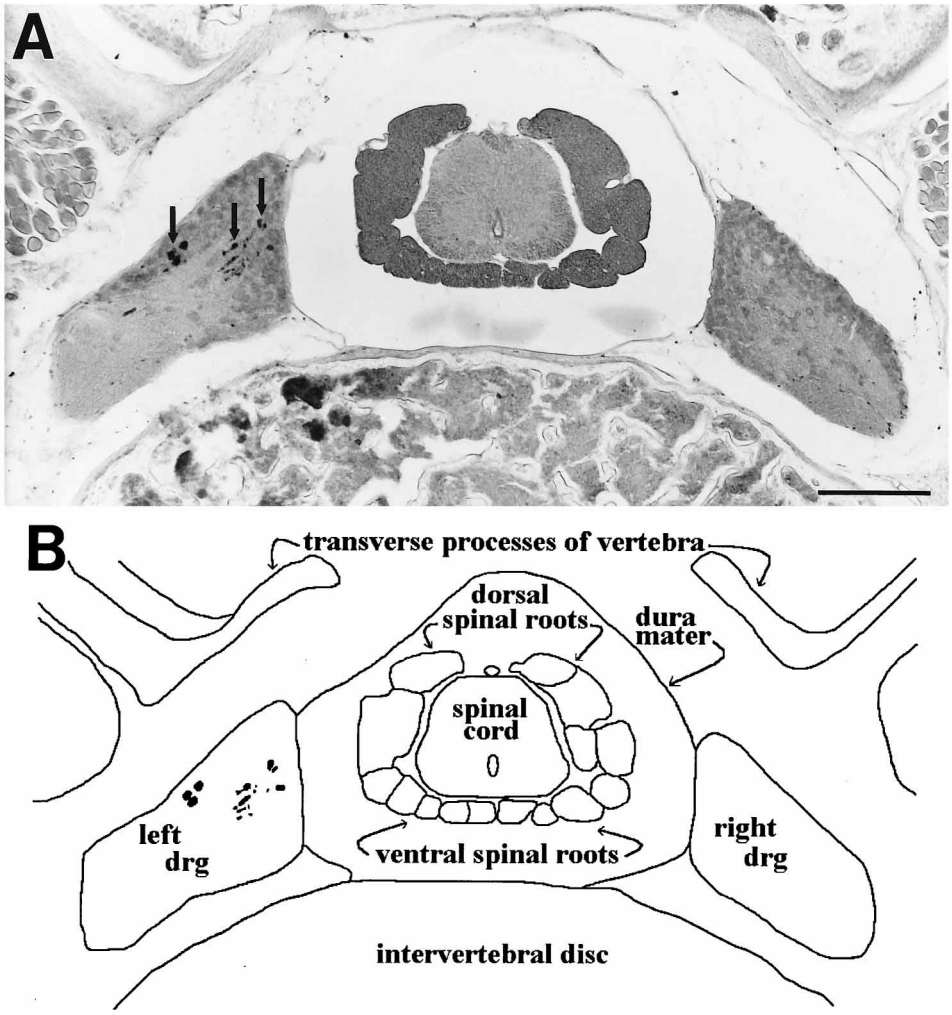

FIG. 1. (A) Low-magnification photomicrograph of an ICC-stained transverse section of the S1 vertebral level of animal 6 (day 4 p.i.), showing the L3 dorsal root ganglia. HSV antigen can be seen in the left dorsal root ganglion (arrows). Bar = 200 μm. (B) Schematic diagram of the photomicrograph, indicating major anatomic landmarks. drg, dorsal root ganglion.

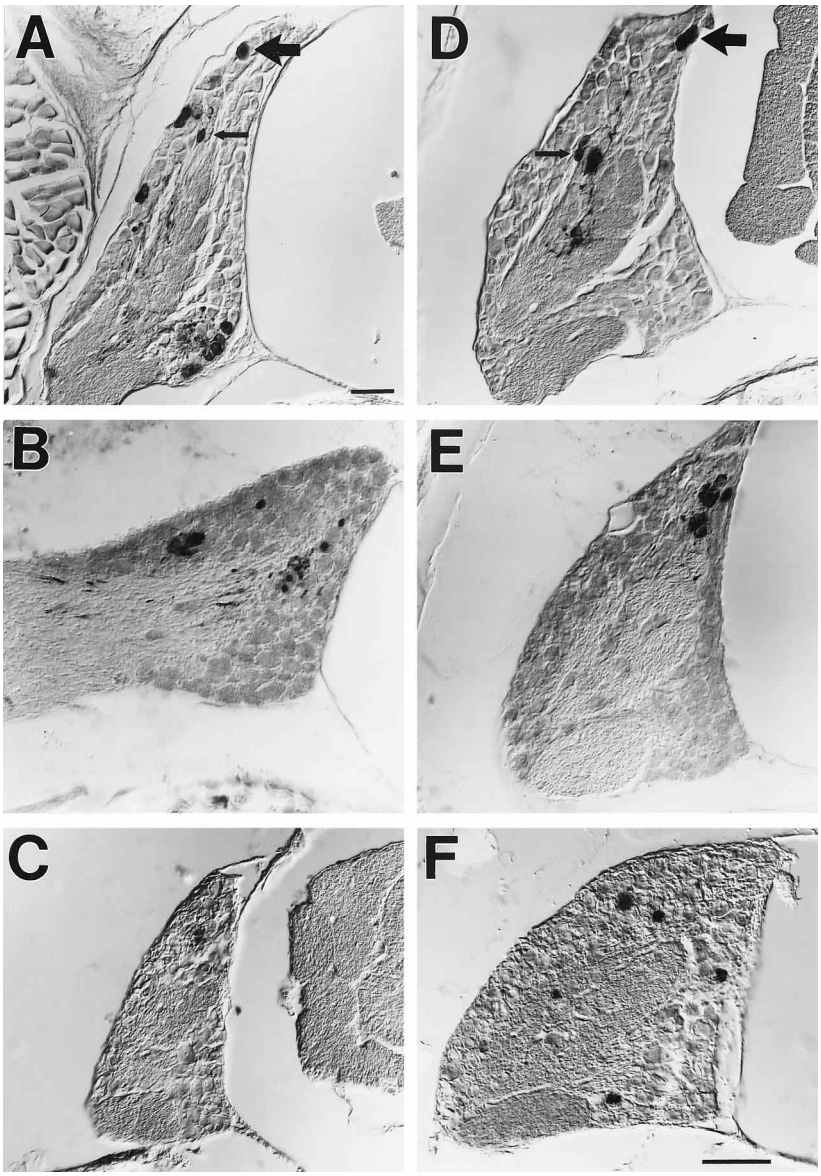

FIG. 2. Time course of HSV antigen deposition in infected left dorsal root ganglia. Representative ICC-stained transverse sections were photographed by using Nomarski illumination. (A, B, and C) Left L3 ganglia of animals 1, 6, and 10, respectively; (D, E, and F) left L2 ganglia of animals 1, 6, and 10, respectively. (A and D) Day 3 p.i.; (B and E) day 4 p.i.; (C and F) day 5 p.i. Large and small arrows indicate infected large- and small-diameter neurons, respectively (see text). Bars = 100 μm.

cells by low-speed centrifugation and disruption of cells by sonication. Viral stock was stored at −70°C, and aliquots were thawed on the day of animal inoculation. Viral titers were determined by standard plaque assays of serial 10-fold dilutions of viral stock in media on monolayers of rabbit skin cells.

Mice and inoculations. Outbred, 5-week-old male Swiss-Webster mice (Simonsen Laboratories, Gilroy, Calif.) were used. After anesthesia with intraperitoneal pentabarbitol (30 to 60 mg/kg) and difluoroethyl-methoxyether inhalation, the glabrous skin of the left hind footpad was gently abraded with an emery board until the stratum corneum was removed so as to not induce bleeding and to ensure that virus was not inoculated into the subdermis. Approximately 0.1 ml of 4 to 80 million PFU (10 to 100 times the previously determined PFU/50% lethal dose for strain 17 *syn*$^+$ in our laboratory [10]) was placed onto the abraded footpad, which was then gently rubbed 5 to 10 times with the shaft of an 18-gauge hypodermic needle. Infected mice were placed in separate cages for analysis on days 3, 4, 5, and 6 p.i. (Table 1).

Animal perfusions and tissue preparation. After heavy sedation with intraperitoneal pentabarbitol (300 mg/kg), animals were transcardially perfused with 0.9% saline followed by modified Bouin's fixative (4% paraformaldehyde, 1% glutaraldehyde, 10% picric acid) with a peristaltic pump. The vertebral spine was removed intact with the spinal cord and dorsal root ganglia in situ from the C1 to S4 level, postfixed for 24 h in modified Bouin's fixative without glutaraldehyde, and decalcified for 4 days in a saturated (approximately 10%) EDTA-water solution, with daily exchanges of the EDTA solution (12). Then spinal columns were placed in 70% ethanol until cleared (usually 4 or 5 days), dehydrated in graded ethanol rinses, cleared in xylene, embedded in paraffin, and sectioned on a rotary microtome. Serial 40 μm-thick tranverse sections of the spinal column, beginning at the S4 vertebral level, were mounted on glass slides. The rostral extent of sectioning depended on the extent of HSV antigen detection. Thus, for day 3 p.i. mice, the sacral and lumbar levels were examined; for day 5 and 6 p.i. mice, the entire vertebral column was sectioned (approximately 5 cm of tissue). For animals 9 and 12 (Table 1), every third section of the spinal column was sampled. The brains of mice with paralysis (animals 10 through 12) were examined. After opening the calvarium, the intact brain stem and brain were removed, placed in modified Bouin's fixative for 24 h, dehydrated, cleared, embedded in paraffin, and sectioned in the coronal plane. Serial 40 μm-thick sections were mounted on glass slides.

Immunocytochemistry (ICC) and microscopy. Mounted sections were deparaffinized in xylene, rehydrated through graded ethanol rinses, equilibrated in phosphate-buffered saline (PBS; 140 mM NaCl, 25 mM KCl, 10 mM Na_2HPO_4, 1.5 mM KH_2PO_4, pH adjusted to 7.4), and incubated in a blocking solution of

TABLE 2. Levels of left dorsal root ganglion HSV antigen detection in asymptomatic mice

Animal no.	Spinal cord levels of detection
1	L4, L3, L2, L1
2	L3, L2
3	L3, L2, L1
4	L3, L2, L1
5	L4, L3
6	L3, L2
7	L3, L2
8	L4, L3, L2
9	ND[a]

[a] ND, not determined.

normal goat serum (1:20 PBS) for 30 min and then for 12 h at 4°C in a solution of primary antibody (rabbit immunoglobulin G raised against HSV-1 MacIntyre strain [Dako Corp., Carpinteria, Calif.]) diluted 1:4,000 in blocking solution. Then sections were rinsed in PBS and incubated in biotinylated goat anti-rabbit secondary antibody and ABC solution by using a commercial kit (ABC Vectastain Elite; Vector Laboratories, Burlingame, Calif.) according to the manufacturer's directions, followed by an immunoperoxidase reaction in filtered 0.05% 3,3′-diaminobenzidine (Sigma, St. Louis, Mo.)–0.03% hydrogen peroxide–PBS solution which stained HSV antigens dark brown. Reactions were monitored by light microscopy. Some sections were counterstained in 0.1% thionin. Photomicroscopy was performed under bright-field illumination with an Olympus Vanox microscope.

Reconstruction. Left-right orientation was maintained throughout processing. Anatomic level was determined by identification of dorsal root ganglia, spinal cord and vertebral body appearance (see Fig. 1), and comparison to an atlas (29). A template of the mouse spinal cord was made from camera lucida drawings of each spinal cord level, and the pattern of infection was plotted on this. Brain stem and spinal cord nuclei and tracts were identified from the atlas (29) and by comparison to previously published neuroanatomic studies of the rodent CNS (3, 15, 22, 23, 27, 28, 31, 33, 34).

RESULTS

The viral inoculum, survival time (p.i.), and clinical disease status of each of the 12 animals examined in this study are summarized in Table 1.

Figure 1 is a low-magnification view of the spinal column at the S1 spinal cord level, providing orientation and identification of the major neural and extraneural structures allowed by the decalcification technique (12). The L3 dorsal root ganglia appear at this level because they are located four vertebral bodies caudal to their corresponding spinal cord level. Thus, dorsal spinal roots eminating from the dorsal root ganglia at the low lumbar and sacrococcygeal spinal cord levels course about 1 cm rostrally within the dura mater before entering the spinal cord. This relatively long rostral-caudal length explains the predominance of the dorsal and ventral roots in transverse sections at this level.

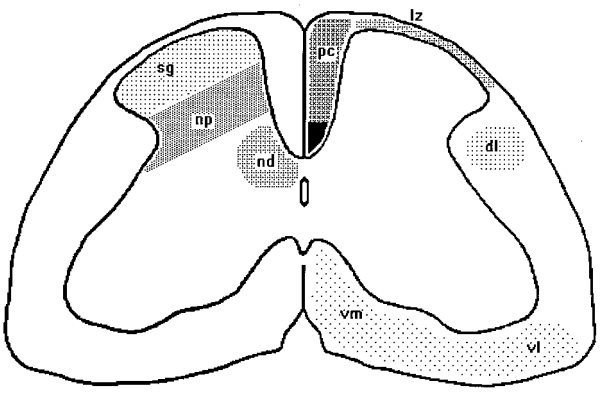

FIG. 3. Schematic representation of the transverse plane of the murine high-lumbar spinal cord, depicting the major regions of HSV antigen detection after hind footpad inoculation. Gray matter area labels are on the left; white matter area labels are on the right. sg, substantia gelatinosa; np, nucleus proprius; nd, nucleus dorsalis; lz, Lissauer's zone; pc, posterior column; dl, dorsolateral; vm, ventromedial; vl, ventrolateral. The dark area in the ventralmost part of the posterior column is the location of the corticospinal tract in rodents (3).

Transneuronal tracing of viral antigen. (i) Dorsal root ganglia and dorsal spinal roots. Dorsal root ganglia were examined on days 3, 4, and 5 p.i. by beginning at the L6 dorsal root ganglia (the S4 spinal cord level) and continuing rostrally until HSV antigen was no longer detected. HSV antigen was most commonly detected in the left L3 and L2 dorsal root ganglia (Fig. 1 and 2; Table 2), with some mice having L4 or L1 involvement (Table 2). HSV antigen was not found in right dorsal root ganglia nor at levels caudal to L4 or rostral to L1. Heaviest HSV antigen detection occurred on day 3, with infection of both large-diameter (50- to 100-μm) and small-diameter (20 to 50-μm) sensory neuron populations (Fig. 2). In determining sensory neuron size, measurements were made on ICC-stained cells which contained nuclei, in addition to examining adjacent sections to rule out measurements made on cells sectioned tangentially. By day 5 p.i., much of the ICC signal had cleared from the infected ganglia.

HSV antigen was detected in the dorsal roots eminating from infected dorsal root ganglia on day 3 p.i. but was limited to the region adjacent to the dorsal root ganglia, just within the CNS. By day 4 p.i., antigen could be traced within the dorsal roots from infected dorsal root ganglia into the CNS and ascending in these roots three or four vertebral levels rostrally. The entry of viral antigen into the spinal cord four vertebral levels rostral to the infected dorsal root ganglion was evident by day 5 p.i.

(ii) Spinal cord. HSV antigen was not detected in the spinal cord until day 5 p.i., and its distribution was related to the presence or absence of clinical symptoms and the level of entry of virus, as determined from infected dorsal root ganglia and dorsal roots. A schematic representation of the major gray and white matter spinal cord regions with HSV antigen detection is depicted in Fig. 3.

Infected gray matter regions were limited to the lumbar and low-thoracic levels primarily in the left dorsal horn (substantia gelatinosa and nucleus proprius) and bilaterally in the region of the nucleus dorsalis (Clark's column), with extensive viral immunoreactivity in symptomatic mice (see Fig. 5). The rostral-caudal extent of gray matter HSV infection was determined by the level of entry of virus at the dorsal root ganglia. Thus, for the day 5 and 6 p.i. animals examined (animals 7 through 12 [Table 1]), dorsal horn gray matter HSV antigen detection was maximal at the L2 and L3 levels (Fig. 4 and 5), corresponding to the commonly infected dorsal root ganglia (Table 2).

Asymptomatic mice examined on day 5 p.i. showed minimal neuropathologic changes. Infected neurons had a preserved cell architecture and the absence of chromatolysis in counterstained sections (Fig. 4). At this stage of infection, transneuronal spread of HSV was most clearly demonstrated, particularly from the posterior column to neurons in the nucleus proprius (Fig. 4C). In contrast to asymptomatic mice, spinal cords from symptomatic mice showed striking neuropathologic changes. In gray matter areas with heavy HSV infection, cell necrosis evidenced by destruction of neuronal-cell architecture and marked chromatolysis was seen (Fig. 5).

Spinal cord white matter involvement in day 5 p.i. asymptomatic mice was limited to the left Lissauer's zone from L3 to

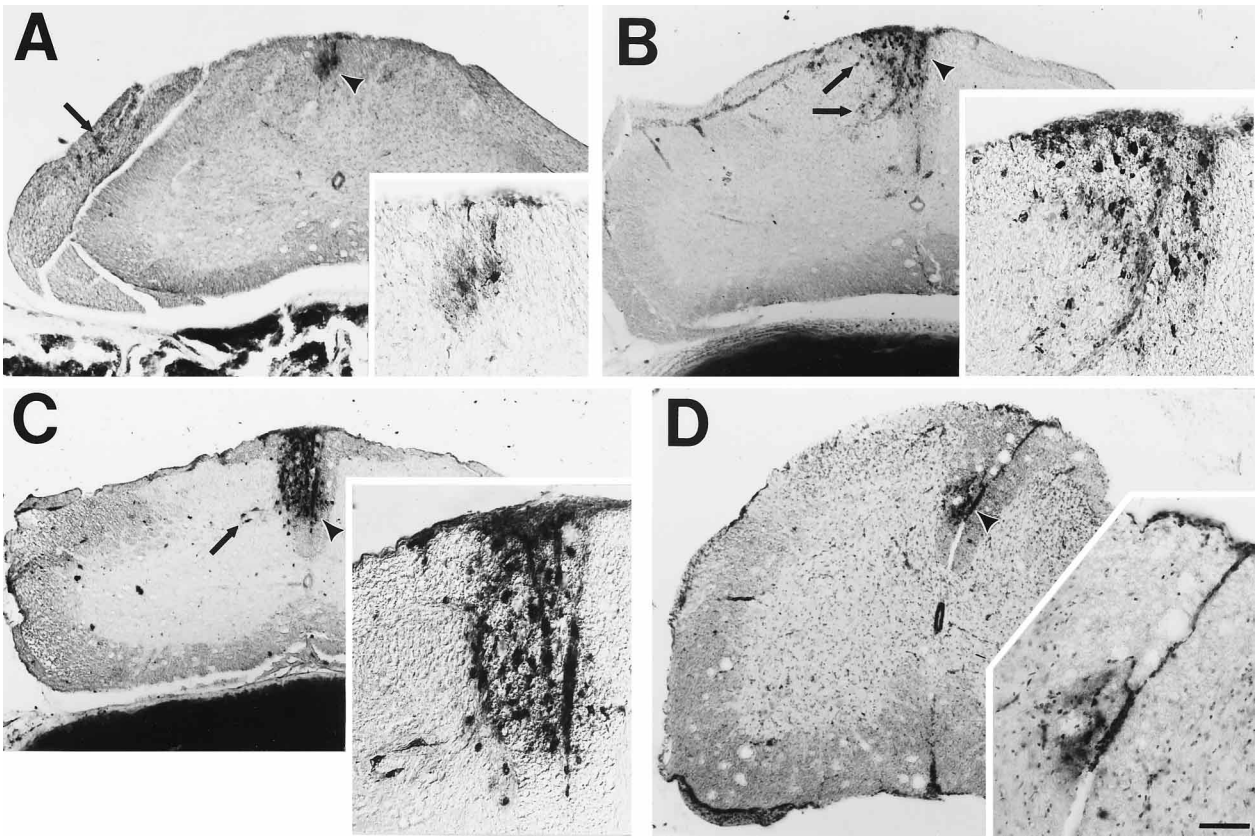

FIG. 4. Representative transverse sections of the lumbar and thoracic spinal cords of day 5 p.i. asymptomatic mice. Sections were ICC stained and lightly counterstained with thionin. (A) L4 level of animal 7, with HSV antigen in the left L3 and L2 dorsal spinal roots (arrow) and posterior column (arrowhead and inset); (B) L3 level of animal 8, with HSV antigen in the region of the posterior column (arrowhead and inset) and spread into substantia gelatinosa and nucleus proprius regions (arrows and inset); (C) L2 level of animal 8, with heavy HSV antigen in the posterior column region (arrowhead and inset) and spread to neurons in the nucleus proprius region (arrow and inset); (D) L1 level of animal 7, with HSV antigen limited to a smaller region of the posterior column (arrowhead and inset) and no detectable gray matter infection. Bar = 100 μm for low-power micrographs and 50 μm for insets.

L2 and the posterior column from L4 to T9 (Fig. 4). No HSV antigen was detected rostral to T8 in these animals. In symptomatic mice, white matter involvement was much more extensive. In the lumbar region, HSV antigen was detected in the left Lissauer's zone and posterior column, bilateral dorsolateral regions, and bilateral ventromedial and ventrolateral regions (Fig. 5). This pattern continued into the thoracic and cervical spinal cord, with the notable spread of HSV antigen to the entire posterior column region at the mid-thoracic level (Fig. 5F). In the cervical cord, HSV antigen deposition in the posterior column was heaviest at the lower third and was no longer detectable at the high cervical levels (Fig. 6). Ventral white matter involvement was decreased in the cervical cord and present predominantly on the right side (Fig. 6). Bilateral dorsolateral white matter HSV antigen was detected throughout the entire cervical cord (Fig. 6).

The spatial distribution of spinal cord gray and white matter HSV antigen deposition in day 5 and 6 p.i. symptomatic mice was plotted on a template from the S1 level to the C1 level (Fig. 6). As expected, sensory regions were the primary target of HSV attack in this model of infection. Despite the paralysis observed in these animals, no evidence of spinal cord motor neuron infection (either in the ventral gray matter alpha motor neurons or the efferent ventral spinal roots) was detected.

(iii) Brain stem and brain. The brains from symptomatic mice were examined to explore whether transneuronal transfer of viral infection into motor pathways occurred at higher levels within the CNS. In all three brains examined (from animals 10 through 12), HSV antigen was detected in the bilateral nucleus subcoeruleus regions at the level of the rostral pons (Fig. 7). No viral antigen was detected in sections rostral to this. Caudal to the rostral pons, HSV antigen was detected in dispersed cells located bilaterally near the midline in the ventral pons (not shown) but went undetected through most of the medulla. Caudal to the decussation of the pyramidal tract, antigen was detected in the pattern shown for C1 in the template (Fig. 6). Because of this gap in antigen detection, it was not possible to definitively trace the transneuronal passage of HSV from the spinal cord to the nucleus subcoeruleus.

DISCUSSION

The purpose of this study was to use the HSV-as-transneuronal-tracer experimental paradigm to explore and define the transneuronal spread phenotype of acute wild-type HSV-1 infection after inoculation of the mouse hind footpad. The data generated here provide a roadmap against which HSV-1 mutants with diminished neuroinvasiveness can be compared. Further, tracer analysis was used to examine how motor nervous system disease (paralysis) develops after a sensory nerve infection.

Using a decalcification technique that did not affect detection of HSV antigen in vivo (12), we were able to trace HSV-1 antigens from the dorsal root ganglia in the peripheral nervous

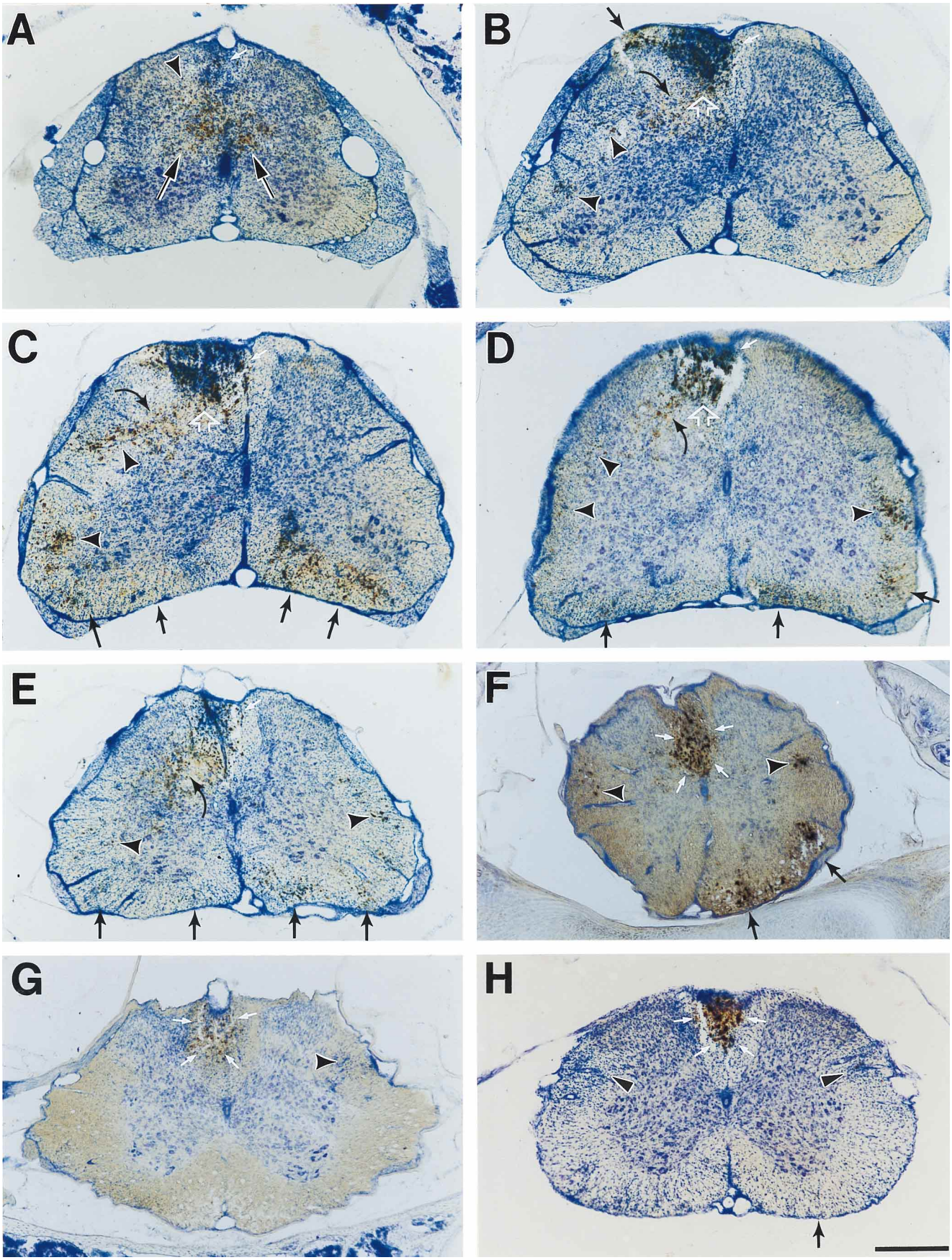

FIG. 5. Representative transverse sections of the lumbar and thoracic spinal cords of day 5 and 6 p.i. symptomatic mice with paralysis (animals 10, 11, and 12). Sections were ICC stained and lightly counterstained with thionin. (A) L4 level of animal 11, demonstrating HSV antigen in the bilateral nucleus dorsalis (arrows) and left nucleus proprius (arrowhead) gray matter regions. These proprioceptive regions were heavily infected one to two segments caudal to the main levels of viral entry

system to the spinal cord without disrupting the normal anatomic relationship of these structures. HSV replication was traced to the first-order neurons in the dorsal root ganglia and to second- and third-order neurons in the spinal cord gray matter. Spinal cord white matter regions containing HSV antigen probably represented virus particles within axons and, thus, detection of viral antigen within supporting neuroglia, such as astrocytes and oligodendrocytes (7, 9, 26, 32–34). It was not the purpose of this study to identify precise cellular localization of HSV within the CNS; however, it should be emphasized that previous ultrastructural studies have clearly shown that neuroglia do not support productive viral replication (1, 9, 26). We infer, therefore, that the ICC staining used in this study detected defective virus particles that others have seen within neuroglia by electron microscopy (1, 9, 26).

Kinetic analysis. The time course of infection in the dorsal root ganglia, spinal roots, and spinal cord correlated well with previously studied replication kinetics of wild-type HSV-1 in these tissues (7, 10, 13, 37). On day 3 p.i., the earliest time point examined, HSV antigen was widely distributed in sciatic nerve roots, dorsal root ganglia neurons, and dorsal roots within the ganglia. On day 4 p.i., infection was primarily seen within the dorsal spinal roots, ascending within the CNS to the point of entry into the spinal cord. Viral antigen was detected in the spinal cord by day 5 p.i., with the extent of infection varying considerably between asymptomatic and symptomatic mice. In symptomatic mice examined on day 5 or 6 p.i., viral antigen had already reached the brain, which was unexpected since in neuroinvasiveness studies, viral replication was not detected until day 7 p.i. (7, 10, 13).

Retrograde transneuronal tracing and transneuronal spread of HSV infection. Comparisons of known neuroanatomical landmarks (3, 8, 22, 23, 27–29, 31) were made to the pattern of HSV antigen deposition observed in the mouse nervous system (Fig. 6). The proposed spinal cord neuronal circuitry involved in HSV infection of the mouse hind footpad is summarized in Fig. 8. We conclude that HSV primarily infected the pathways of the sensory modalities, which was the result of invasion of virus into sensory nerve terminals present in the richly innervated glabrous skin of the hind footpad.

Somatotopic projection of HSV antigen from the hind footpad to the nervous system. HSV antigen was detected in first- and second-order neurons projecting to the skin of the hind footpad. Thus, antigen was detected primarily in the L3 and L2 dorsal root ganglia (Table 2) supplied by the tibial branch of the sciatic nerve which innervates the hind footpad dermatome (28, 31). The somatotopic representation of this dermatome was traced into the spinal cord by plotting the distribution of HSV antigen in substantia gelatinosa at the L3 and L2 levels (Fig. 6). The pattern of viral replication in these second-order neurons corresponded well to earlier studies of somatotopic mapping of sciatic nerve branches in the rat using traditional tracers (23, 28, 31).

The nociceptive pathway. Cutaneous receptors of nociception that respond to painful thermal and mechanical stimuli utilize both large myelinated (Aδ) and small unmyelinated (C) fibers. The Aδ and C fibers are axons of the large- and small-diameter bipolar neurons, respectively, of the dorsal root ganglion (25). Both populations of neurons were infected by HSV-1 in this experiment (Fig. 2), which we interpret as indicative of retrograde spread from cutaneous nociceptor terminals in the footpad to the cell bodies of the dorsal root ganglia. Intense HSV infection peaked at days 3 and 4 p.i. and correlated well with the known peak of viral replication that occurs in dorsal root ganglia neurons (7, 10).

HSV antigen was then traced into the spinal roots eminating from infected dorsal root ganglia to where these roots enter the spinal cord. From the L3 level to the L1 level, second-order neurons of nociception that reside in the substantial gelatinosa region of the spinal cord gray matter were labelled in day 5 and 6 p.i. animals. In symptomatic mice, HSV antigen extended into the deeper layers of substantia gelatinosa neurons, representing third-order viral replication. We conclude that at least some of these infected third-order neurons give rise to axons which comprise the ascending spinothalamic tract. This conclusion is supported by the detection of viral antigen, beginning at the L2 level, in the bilateral ventromedial and ventrolateral white matter regions (Fig. 5). Further, infection was more intense in the right ventral white matter corresponding to the crossed fibers that make up 90% of the spinothalamic tract. The rostral extent of ventral white matter viral antigen detection was to the C1 level, but viral antigen was not detected higher in the brain stem or brain in the three symptomatic mice probably because of the examination time of day 5 or 6 p.i., with viral replication peaking in the brain at day 9 p.i. (7, 10, 13).

The proprioceptive pathways. The cutaneous receptors of proprioception in glabrous skin respond to mechanical stimuli such as position and pressure sensation. These receptors are comprised primarily of myelinated Aδ fibers eminating from large-diameter sensory neurons in the dorsal root ganglia (24). In infected dorsal root ganglia at all the time points examined, the predominant cells with HSV antigen deposition were the large-diameter population of sensory neurons (Fig. 2). We

at L2 and L3. Viral antigen was also detected in the left posterior column region (white arrow), the only white matter area infected at the L4 level. (B) L3 level of animal 10, with dense HSV antigen deposition, marked necrosis, and chromatolysis in the left dorsal horn nociceptive regions (Lissauer's zone and substantia gelatinosa [open white arrow]) and proprioceptive region (nucleus proprius [curved arrow]). The entry of HSV antigen is seen in the left L3 dorsal spinal root (arrow) which eminated from the L3 dorsal root ganglia at the S1 vertebral level (Fig. 1). White matter infection was evident in the left posterior column (white arrow) and the left dorsolateral white matter region (arrowheads) in the location of the ascending spinocerebellar tract. (C) L2 level of animal 10, showing a pattern in the left dorsal horn gray matter nociceptive (open white arrow) and proprioceptive (curved arrow) regions similar to that seen at level L3. HSV antigen in white matter regions was detected in the left posterior column (white arrow), left dorsolateral and dorsoventral regions (arrowheads), and bilateral ventromedial and ventrolateral white matter regions (arrows). In the latter, antigen deposition was heavier on the right side, contralateral to the side of inoculation, consistent with the decussation of the majority of spinothalamic tract fibers from infected L2 and L3 dorsal horn spinothalamic tract neurons. (D) L1 level of animal 10, showing HSV antigen detection in the left dorsal horn, with gray matter infection limited to the medial aspect of the substantia gelatinosa (open white arrow) and the nucleus proprius (curved arrow). Heavy posterior column infection was still present (white arrow) where severe necrosis resulted in tissue separation on the microtome. White matter infected regions begin to predominate at the L1 level, with HSV antigen in bilateral ventrolateral and ventromedial regions (arrows) primarily on the right side and bilateral dorsolateral regions (arrowheads). (E) T12 level of animal 10, demonstrating near clearing of HSV antigen in the left dorsal horn gray matter with infection limited to the left nucleus proprius region (curved arrow). White matter involvement was evident in the left posterior column (white arrow), bilateral dorsolateral regions (arrowheads), and right-greater-than-left ventrolateral and ventromedial regions (arrows). (F) T9 level of animal 10, demonstrating HSV antigen detection in white matter regions. Extensive infection was evident in the posterior column (white arrows). HSV antigen was detected in bilateral dorsolateral regions (arrowheads) and the right ventrolateral and ventromedial regions (arrows); left ventral white matter involvement was no longer evident. (G) T3 level of animal 12, demonstrating continued infection in the posterior column (white arrows) and in the right dorsolateral region (arrowhead). (H) T1 level of animal 11, with HSV antigen detected in the posterior column (white arrows), bilateral dorsolateral white matter regions (arrowheads), and right ventral white matter (arrow). Bar = 100 μm.

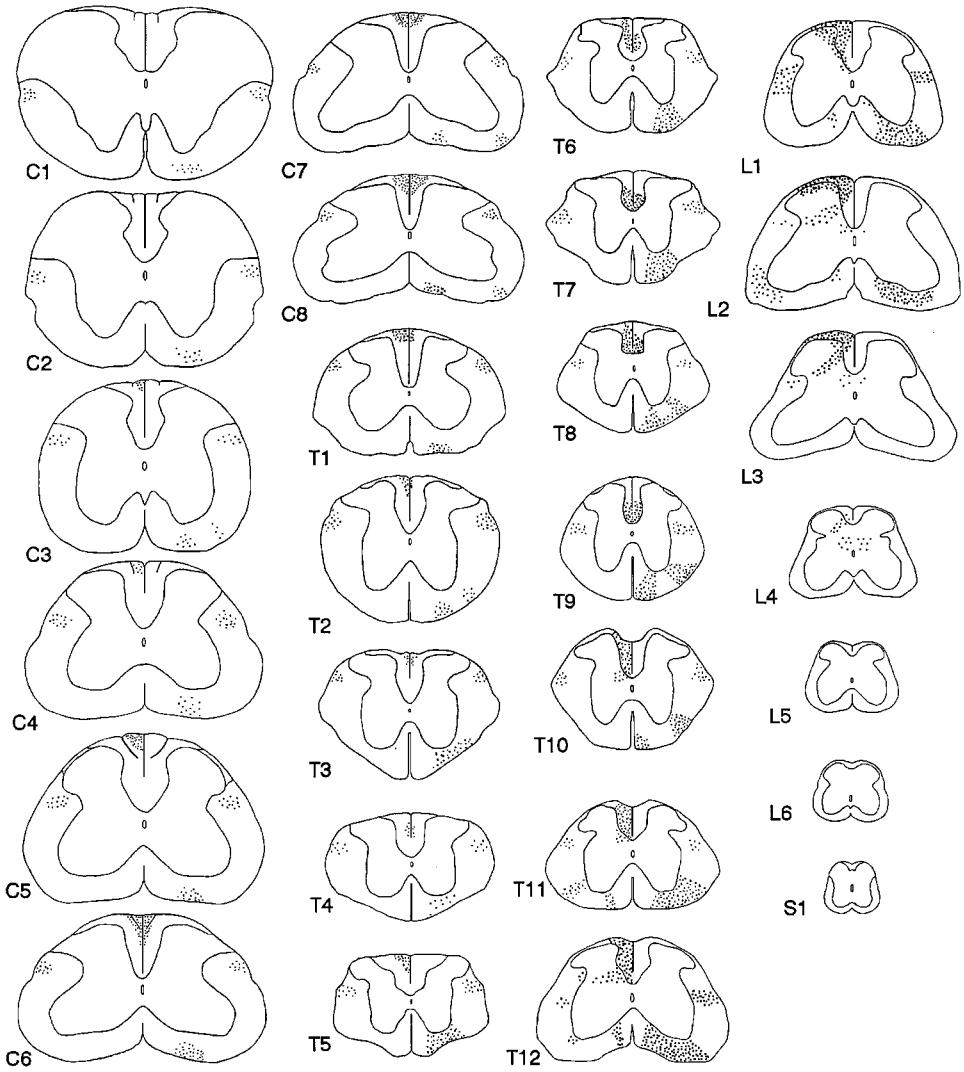

FIG. 6. Spinal cord template from S1 to C1, with gray and white matter boundaries shown. HSV antigen was plotted at each level for day 5 and 6 p.i. symptomatic mice. The data summarize the results for animals 10 through 12 (Table 1).

interpret this finding as indicative of efficient viral neuroinvasion of cutaneous receptors of proprioception present in the hind footpad.

Further evidence of extensive transsynaptic spread of HSV within the proprioceptive pathway was evident in the spinal cord. Unlike the nociceptive spinothalamic pathway, proprioceptive circuits within the spinal cord consist of two anatomically distinct pathways, (i) the short and intermediate fibers that enter and terminate in the nucleus proprius and the nucleus dorsalis regions of the spinal cord gray matter at the segment of entry and two to three segments rostral and caudal to the entry segment and (ii) the long fibers that make up the gracile fasciculus of the posterior column. The nucleus dorsalis neurons give rise to axons that make up the uncrossed ascending dorsal spinocerebellar tract, and the long fibers of the gracile fasciculus ascend in the posterior column, eventually terminating in the gracile nucleus in the medulla (Fig. 8).

All three regions of spinal cord gray and white matter corresponding to these propriceptive pathways were found to contain HSV antigen. First, neurons in the region of the nucleus proprius and nucleus dorsalis from the L4 through T10 levels were infected (Fig. 4 and 5). In both nuclei, HSV antigen spread was bilateral in symptomatic animals. Second, HSV antigen was traced bilaterally to the dorsolateral white matter regions corresponding to the uncrossed ascending dorsal spinocerebellar tract whose axons originate from nucleus dorsalis neurons. The dorsal spinocerebellar tract was labelled from the midlumbar region through the cervical spinal cord levels in symptomatic animals (Fig. 5 and 6). Third, the posterior column containing the gracile fasciculus had widespread HSV antigen deposition from the L4 level to the C3 spinal cord level (Fig. 6). Infection was not detected further rostrally in the symptomatic mice, again probably due to the examination time selected in this study, which was several days prior to peak viral replication in the brain.

Motor nervous system involvement. Direct sensory-to-motor-system transneuronal spread of HSV-1 infection was not evident in this study. The paralysis that developed in infected mice at day 5 and 6 p.i. could not be explained by the pattern of HSV spinal cord involvement of the sensory modality pathways, as described above. Further, HSV antigen deposition and neuropathology were not detected in alpha motor neurons in

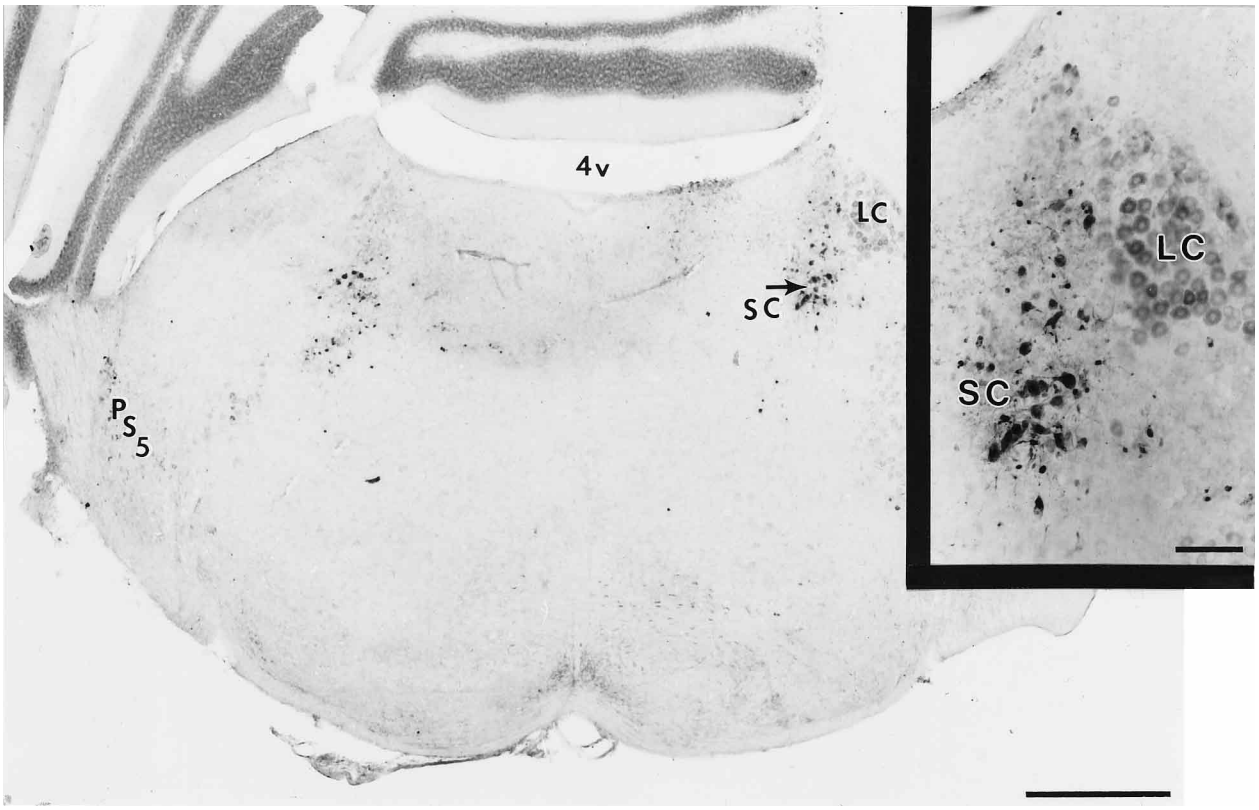

FIG. 7. Representative coronal section, without counterstain, at the level of the rostral pons of animal 12, showing HSV antigen detection in bilateral nucleus subcoeruleus (SC) neurons (arrow and inset). The locus coeruleus (LC), principle sensory nucleus of the fifth cranial nerve (PS5), and the fourth ventricle (4v) are labelled for orientation. Bar = 500 μm; inset bar = 100 μm.

the ventral gray matter of the spinal cord or in ventral spinal roots eminating from the cord. One possibility is that paralysis resulted from the severe myelitis present in sensory regions of the lumbar spinal cord (Fig. 5A through D) via interruption of interneuronal pathways within the cord. However, viral immunoreactivity was not detected in classic spinal cord reflex connections between the dorsal and ventral spinal cord nuclei.

Another possibility is that sensory-to-motor transneuronal transfer of viral infection occurred at higher levels of the CNS. Ugolini et al. (33) injected HSV-1 directly into the ulnar and median nerves of the rat forelimb and detected transneuronal spread into many brain stem loci in late stages of infection. To test this hypothesis in our model, we examined the brains of the three paralyzed animals in this study. HSV infection was detected in the bilateral nucleus subcoeruleus of the pons (Fig. 7), a region not known to be involved in motor function. This nucleus is a major contributor of noradrenergic input into sensory regions of the spinal cord and participates in the modulation of spinal nociceptive transmission (15). Thus, our result is consistent with retrograde transneuronal transfer of HSV infection to a higher-order neuron population of the sensory nervous system. Nucleus subcoeruleus efferent axons have been traced the full length of the spinal cord and decussate at all levels (reviewed in reference 15). Ugolini et al. (33) also detected HSV in this region bilaterally after unilateral inoculation, but because their system involved inoculation of both motor and sensory nerves, more widespread infection was detected in the brain stem. We could not definitively trace the spinal cord pathway to the nucleus subcoeruleus infection because of the gap in antigen detection through the medulla. However, because bilateral antigen detection was seen in the dorsolateral columns through the C1 level (Fig. 6) and because of previous neuroanatomic studies of this pathway (15), it is likely that the nucleus subcoeruleus neurons were infected from tracts located in the dorsolateral region of the spinal cord.

An alternative explanation of hindlimb paralysis is that it occurred via nontranssynaptic spread of HSV infection. In rodents, the descending corticospinal tract traverses the ventralmost part of the posterior column (3) (Fig. 3 and 8); this tract appeared to be heavily infected with HSV, particularly at the midthoracic spinal cord level (Fig. 5F). Corticospinal tract involvement may have resulted from extension of the adjacent heavily infected long fibers of proprioception (the gracile fasciculus), perhaps by disruption of normal neurotransmission from surrounding gliosis. Supporting this hypothesis was the observation (not shown) that mice with bilateral paralysis had corresponding bilateral posterior column infection in the thoracolumbar cord, whereas mice with unilateral paralysis had unilateral posterior column infection.

Our hypothesis of motor involvement through nontranssynaptic spread of virus-induced pathology within neuroglia of the posterior column may be in conflict with studies demonstrating that neuroglia support only abortive viral replication (1, 6, 9). Notably, Card et al. (6) studied vagus nerve pathways after inoculation of the stomach wall of the rat with PrV. In their detailed ultrastructural and ICC analysis through the dorsal motor vagus complex in the rat brain stem, they demonstrated that PrV replicated only within synaptically connected neurons, that nonneuronal infection (glia and resident macro-

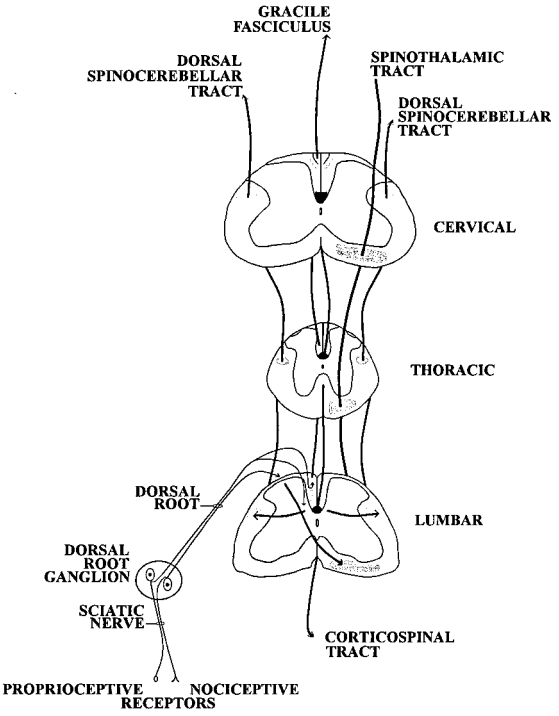

FIG. 8. Schematic diagram that summarizes the proposed transneuronal passage of HSV-1 after hind footpad inoculation. Viral infection primarily involved the ascending sensory pathways of nociception and proprioception. Infection was detected in first-order neurons of the dorsal root ganglia and traced into the dorsal roots until their entry into the corresponding spinal cord level. In the cord, infection was detected in second-order neurons of nociception and proprioception. Nociceptive neurons in the substantia gelatinosa spread infection to third-order spinothalamic tract neurons whose axons primarily cross to the right side and ascend in the spinothalamic tract located in the ventrolateral and ventromedial white matter regions. Second-order proprioceptive neurons were in two locations, the nucleus dorsalis and nucleus proprius. Bilateral nucleus dorsalis infection resulted in spread to third-order dorsal spinocerebellar tract neurons whose axons ascend bilaterally in dorsolateral white matter regions. Heavy infection of proprioceptive first-order neurons in the dorsal root ganglia also involved bipolar populations whose axons comprise the long tract fibers of the gracile fasciculus, ascending in the posterior column. The descending corticospinal tract is shown in the ventralmost portion of the posterior column, adjacent to the gracile fasciculus (3). It is postulated that this motor nervous system region was involved by nontranssynaptic spread from the gracile fasciculus and may have caused the hindlimb paralysis observed late in infection.

phages) supported only abortive replication, and that these cells functioned to restrict viral spread to the neuronal circuitry determined by the site of inoculation. Thus, confirmation of our hypothesis of motor nervous system involvement in the mouse CNS will require a similar ultrastructural analysis of the posterior column of the thoracolumbar spinal cord.

Conclusion. Our data support the findings of a recent tracer experiment which analyzed HSV antigen deposition in the spinal cord of rats after mixed-nerve inoculation (34). In that study, HSV-1 was inoculated directly onto the exposed tibial (hindlimb) or median (forelimb) nerves and viral antigen was traced to sensory, motor, and autonomic circuits within the spinal cord. Our model of infection enabled analysis of pure sensory neuronal circuitry, a situation which exists in most human HSV infections. Further, the decalcification technique used here preserved the normal anatomic positions of the dorsal root ganglia, spinal roots, and spinal cord, enabling accurate transneuronal tracing from the peripheral nervous system to the CNS.

The present study provides the baseline data against which the neuroinvasiveness and transneuronal spread phenotypes of HSV mutants can be explored in the mouse hind footpad inoculation model of infection. The alphaherpesvirus-as-transneuronal-tracer experimental paradigm has been used recently to study the attenuated neuropathogenesis of a PrV vaccine strain compared to that of the highly neurovirulent wild-type PrV (4, 5, 35). Using the rat retina inoculation model, marked differences in the transneuronal spread of virus within the CNS visual circuitry were demonstrated (4). The attenuated phenotype of the vaccine strain was mapped to two PrV surface glycoprotein genes (5, 35). Thus, the traditional virologic phenotype of neuroinvasiveness, complemented with the phenotype of transneuronal spread, has greatly enhanced our understanding of how various viral gene products function to effect the neuropathogenesis of alphaherpesvirus infection.

REFERENCES

1. **Bak, I. J., C. H. Markham, M. L. Cook, and J. G. Stevens.** 1977. Intraaxonal transport of *herpes simplex* virus in the rat central nervous system. Brain Res. **136:**415–429.
2. **Bak, I. J., C. H. Markham, M. L. Cook, and J. G. Stevens.** 1978. Ultrastructural and immunoperoxidase study of striatonigral neurons by means of retrograde axonal transport of herpes simplex virus. Brain Res. **143:**361–368.
3. **Brown, L. T.** 1971. Projections and termination of the corticospinal tract in rodents. Exp. Brain Res. **13:**432–450.
4. **Card, J. P., M. E. Whealy, A. K. Robbins, R. Y. Moore, and L. W. Enquist.** 1991. Two α-herpesvirus strains are transported differentially in the rodent visual system. Neuron **6:**957–969.
5. **Card, J. P., M. E. Whealy, A. K. Robbins, and L. W. Enquist.** 1992. Pseudorabies virus envelope glycoprotein gI influences both neurotropism and virulence during infection of the rat visual system. J. Virol. **66:**3032–3041.
6. **Card, J. P., L. Rinaman, R. B. Lynn, B.-H. Lee, R. P. Meade, R. R. Miselis, and L. W. Enquist.** 1993. Pseudorabies virus infection of the rat central nervous system: ultrastructural characterization of viral replication, transport, and pathogenesis. J. Neurosci. **13:**2515–2539.
7. **Cook, M. L., and J. G. Stevens.** 1973. Pathogenesis of herpetic neuritis and ganglionitis in mice: evidence for intra-axonal transport of infection. Infect. Immun. **7:**272–288.
8. **Edgley, S. A., and C. M. Gallimore.** 1988. The morphology and projections of dorsal horn spinocerebellar tract neurones in the cat. J. Physiol. **397:**99–111.
9. **Field, H. J., and T. J. Hill.** 1974. The pathogenesis of pseudorabies in mice following peripheral inoculation. J. Gen. Virol. **23:**145–157.
10. **Goodman, J. L., and J. P. Engel.** 1991. Altered pathogenesis in herpes simplex virus type 1 infection due to a syncytial mutation mapping to the carboxy terminus of glycoprotein B. J. Virol. **65:**1770–1778.
11. **Goodpasture, E. W., and O. Teague.** 1923. Transmission of the virus of herpes febrilis along nerves in experimentally infected rabbits. J. Exp. Med. **44:**139–184.
12. **Henken, D. B., and J. R. Martin.** 1993. Neural antigen detection in mouse tissues is not impaired by decalcification. Acta Neuropathol. **86:**176–178.
13. **Izumi, K. M., and J. G. Stevens.** 1990. Molecular and biological characterization of a herpes simplex virus type 1 (HSV-1) neuroinvasiveness gene. J. Exp. Med. **172:**487–496.
14. **Johnson, R. T.** 1964. The pathogenesis of herpes virus encephalitis. I. Virus pathways to the nervous system of suckling mice demonstrated by fluorescent antibody staining. J. Exp. Med. **119:**343–356.
15. **Jones, S. L.** 1991. Descending noradrenergic influences on pain. Prog. Brain Res. **88:**381–394.
16. **Krinke, G. J., and F. M. Dietrich.** 1990. Transneuronal spread of intraperitoneally administered herpes simplex virus type 1 from the abdomen via the vagus nerve to the brains of mice. J. Comp. Pathol. **103:**301–306.
17. **Kristensson, K.** 1970. Morphologic studies of the neural spread of herpes simplex virus to the central nervous system. Acta Neuropathol. **16:**54–63.
18. **Kristensson, K., A. Vahlne, L. A. Persson, and E. Lycke.** 1978. Neural spread of herpes simplex virus types 1 and 2 in mice after corneal or subcutaneous (footpad) inoculation. J. Neurol. Sci. **35:**331–340.
19. **Kristensson, K., I. Nenessmo, L. Persson, and E. Lycke.** 1982. Neuron to neuron transmission of herpes simplex virus. Transport of virus from skin to brainstem nuclei. J. Neurol. Sci. **54:**149–156.
20. **Kuypers, H. G. J. M., and G. Ugolini.** 1990. Viruses as transneuronal tracers. Trends Neurosci. **13:**71–75.
21. **McKendall, R. R.** 1980. Comparative neurovirulence and latency of HSV_1 and HSV_2 following footpad inoculation of mice. J. Med. Virol. **5:**25–32.
22. **Molander, C., Q. Xu, and G. Grant.** 1984. The cytoarchitectonic organization of the spinal cord in the rat. I. The lower thoracic and lumbosacral cord. J. Comp. Neurol. **230:**133–141.
23. **Molander, C., and G. Grant.** 1985. Cutaneous projections from the rat

hindlimb foot to the substantia gelatinosa of the spinal cord studied by transganglionic transport of WGA-HRP conjugate. J. Comp. Neurol. **237:** 476–484.

24. **Norgren, R. B., Jr., and M. N. Lehman.** 1989. Retrograde transneuronal transport of herpes simplex virus in the retina after injection in the superior colliculus, hypothalamus and optic chasm. Brain Res. **479:**374–378.
25. **Ranson, S. W.** 1912. The structure of the spinal ganglia and of the spinal nerves. J. Comp. Neurol. **22:**159–175.
26. **Rinaman, L., J. P. Card, and L. W. Enquist.** 1993. Spatiotemporal responses of astrocytes, ramified microglia, and brain macrophages to central neuronal infection with pseudorabies virus. J. Neurosci. **13:**685–702.
27. **Rivero-Melián, C., and G. Grant.** 1990. Lumbar dorsal root projections to spinocerebellar cell groups in the rat spinal cord: a double label study. Exp. Brain Res. **81:**85–94.
28. **Rivero-Melián, C., and G. Grant.** 1990. Distribution of lumbar dorsal root fibers in the lower thoracic and lumbosacral spinal cord of the rat studied with choleragenoid horseradish peroxidase conjugate. J. Comp. Neurol. **299:** 470–481.
29. **Sidman, R. L., J. B. Angevine, Jr., and E. T. Pierce.** 1971. Atlas of the mouse brain and spinal cord. Harvard University Press, Cambridge, Mass.
30. **Stevens, J. G.** 1993. HSV-1 neuroinvasiveness. Intervirology **35:**152–163.
31. **Swett, J. E., and C. F. Woolf.** 1985. The somatotopic organization of primary afferent terminals in the superficial laminae of the dorsal horn of the rat spinal cord. J. Comp. Neurol. **231:**66–77.
32. **Ugolini, G., H. G. J. M. Kuypers, and A. Simmons.** 1987. Retrograde transneuronal transfer of herpes simplex virus type 1 (HSV 1) from motoneurones. Brain Res. **422:**242–256.
33. **Ugolini, G., H. G. J. M. Kuypers, and P. L. Strick.** 1989. Transneuronal transfer of herpes virus from peripheral nerves to cortex and brainstem. Science **243:**89–91.
34. **Ugolini, G.** 1992. Transneuronal transfer of herpes simplex virus type 1 (HSV-1) from mixed limb nerves to the CNS. I. Sequence of transfer from sensory, motor, and sympathetic nerve fibres to the spinal cord. J. Comp. Neurol. **326:**527–548.
35. **Whealy, M., J. P. Card, A. K. Robbins, J. R. Dubin, H.-J. Rziha, and L. W. Enquist.** 1993. Specific pseudorabies virus infection of the rat visual system requires both gI and gp63 glycoproteins. J. Virol. **67:**3786–3797.
36. **Wildy, P.** 1967. The progression of herpes simplex virus to the central nervous system of the mouse. J. Hyg. Camb. **65:**173–192.
37. **Yuhasz, S. A., and J. G. Stevens.** 1993. Glycoprotein B is a specific determinant of herpes simplex virus type 1 neuroinvasiveness. J. Virol. **67:**5948–5954.